51. Cr-SPINEL AS A PETROGENETIC INDICATOR: DEDUCING MAGMA COMPOSITION FROM SPINELS IN HIGHLY ALTERED BASALTS FROM THE JAPAN SEA, SITES 794 AND 797[1]

James F. Allan[2]

ABSTRACT

Cr-rich spinels obtained from drill cores in the margins of heavily altered basaltic sills and flows contain a wealth of petrological information about the host magmas that crystallized them. These host igneous units, cored during Leg 127 of the Ocean Drilling Program in the Japan Sea, underwent extensive hydrothermal alteration that makes petrogenetic interpretations difficult. Most spinels in these samples exhibit minor or no zoning and are similar in composition to others reported from mid-ocean ridge basalt and backarc basin basalt tholeiites. Most show a range in $Cr/(Cr + Al)$ of 0.26 to 0.62, a range in $Mg/(Mg + Fe^{2+})$ of 0.53 to 0.68, low TiO_2 ($<0.7\%$), and low $Fe^{3+}/(Cr + Al + Fe^{3+})$ (<0.1), which is consistent with crystallization from a tholeiitic liquid at a magmatic oxygen fugacity 2 log units or more below the nickel–nickel oxide oxygen buffer. By recasting the composition of these spinels in terms of an ideal reciprocal solution model and by deriving a ΔG_{EX}° for spinel-liquid Mg-Fe^{2+} exchange, direct determination of magmatic $Mg/(Mg + Fe^{2+})$ is possible. The compositions of these Leg 127 spinels clearly show that some units underwent syn- and post-eruption enrichment in $Mg/(Mg + Fe^{2+})$ during hydrothermal alteration and diagenesis. This study proves that Cr-spinel is a unique and powerful tool for deciphering the original magmatic characteristics of heavily altered basalts.

INTRODUCTION

Cr-rich spinel within basaltic lavas is a proven tool for deciphering petrogenetic history. The complex crystal chemistry of Cr-spinel (e.g., Sack and Ghiorso, 1991a, 1991b; Sack, 1982; Irvine, 1976) makes its composition a sensitive indicator of intensive and extensive magmatic variables (Irvine, 1965, 1967). Cr-spinel is a particularly sensitive indicator of melt disequilibria, typically exhibiting ranges in composition an order of magnitude larger than the silicate melts from which it crystallizes (Allan, Sack, and Batiza, 1988). Inferences regarding magma mixing (Roeder and Reynolds, 1991; Allan, Sack, and Batiza, 1988; Natland et al., 1983), initiation of precipitation of coexisting phases (Fisk and Bence, 1980; Foruta and Tokuyama, 1983; Dick and Bullen, 1984), the chemical evolution of a lava lake (Scowen et al., 1991), and identification of different liquid lines of descent (Natland, 1989) have been made from variations in basalt Cr-spinel composition. Spinel chemistry has also been used to deduce information about fO_2 (Fisk and Bence, 1980; Batiza and Vanko, 1984; Hawkins and Melchior, 1985), and temperature (Fisk and Bence, 1980) during crystallization. Allan, Sack, and Batiza (1988) advanced the use of Cr-spinel as a petrogenetic indicator for basaltic liquids by directly solving for melt-spinel Mg-Fe^{2+} exchange equilibria, making it possible to determine whether a given spinel was in equilibrium with a given silicate liquid. In this paper, original magmatic compositions of altered basaltic sills and flows are inferred from Cr-spinel compositions from samples collected by the drillship *JOIDES Resolution* during Leg 127 of the Ocean Drilling Program (ODP) in the Japan Sea.

The Japan Sea, one of several marginal basins that lie at the western edge of the Pacific Ocean, generally is understood to have formed by the rifting of a continental volcanic arc in the mid-Tertiary (Tamaki, Pisciotto, Allan, et al., 1990; Tamaki, 1985; Celaya and McCabe, 1987; Hilde and Wageman, 1973; Karig, 1971, 1974; Lallemand and Jolivet, 1987). A primary goal of Leg 127 was to determine the nature and age of the crust underlying this backarc basin and also to determine its spreading history. The Japan Sea consists of the Yamato and Japan basins, which are separated by the rifted continental crust of the Yamato Rise (Fig. 1). Basement coring during Leg 127 focused on two sites within the

Yamato Basin: one at the western basinal margin (Site 797) and one roughly in the northern center of the basin (Site 794). Basement at Site 794 was recored during Leg 128, which extended recovery to a deeper level than Leg 127 (Ingle, Suyehiro, von Breymann, et al., 1990).

A major finding of both legs was that sediment/basaltic sill complexes make up the uppermost crust of the Yamato Basin. Backarc extension proceeded in the Yamato Basin from 19 to 15.5 Ma, producing tholeiitic magmas at both Sites 794 and 797 (Tamaki, Pisciotto, Allan, et al., 1990). Knowledge of the chemistry of the melts that formed the sills is crucial toward understanding the spreading dynamics and thermal regime that produced the Japan Sea backarc basin, yet the rock samples collected in the drill cores are typically moderately to very highly altered. Many of the major elements, especially Mg, Ca, Na, and K, were mobile during the hydrothermal alteration that occurred as the sills were emplaced into soft sediment, and vital magmatic parameters, $Mg/(Mg + Fe^{2+})$ in particular, have been significantly affected (Allan and Gorton, this volume; Tamaki, Pisciotto, Allan, et al., 1990). As a result, accurate liquid line of descent calculations for the collected suite are simply not possible.

In the heavily altered margins of these igneous units, only magmatic Cr-spinel has been preserved. The goal of this chapter is to infer primary magmatic compositional characteristics from these spinel compositions. These characteristics include the following: (1) magmatic $Mg/(Mg + Fe^{2+})$, derived from explicitly solving for Mg-Fe^{2+} liquid-spinel exchange equilibria; (2) magmatic fO_2; and 3) liquid-spinel disequilibria, which give evidence for magma mixing of disparate magmas.

PETROGRAPHY AND CHEMISTRY OF HOST ROCKS

Coring during Leg 127 recovered six igneous units at Site 794 and 21 igneous units at Site 797. Nearly all of these units represent sills intruded into soft, tuffaceous, and silty claystones at Site 794 and soft, interlaminated sandstones, siltstones, and silty claystones at Site 797. This interpretation is based on the following: (1) the presence of baked sediments above and below unit margins (including welding of tuffaceous sediments and the reversal of sediment magnetic orientation); (2) the massive and thick nature of the units (10–40 m for most units); (3) the fining of unit grain size, from coarse doleritic or basaltic interiors to fine-grained basalts on the unit margins; (4) the lack of
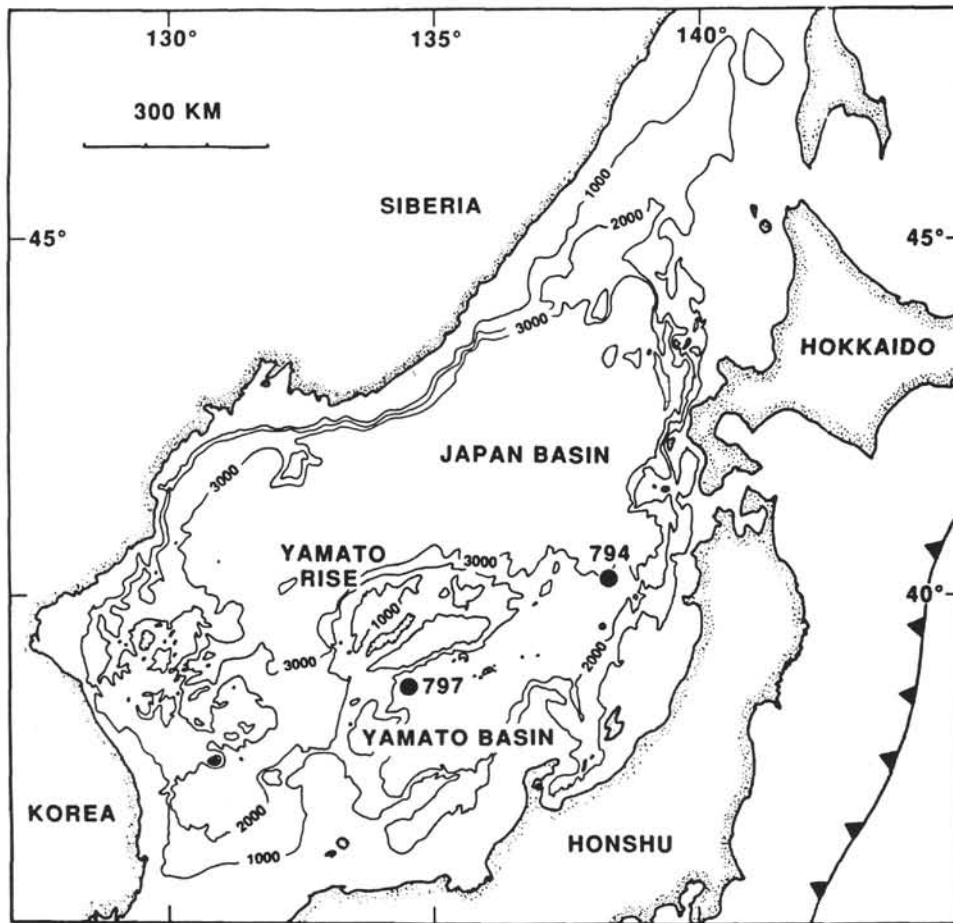

Figure 1. Location map showing the sites cored during Leg 127 which contained Cr-spinel-bearing units.

rubbly zones at the unit margins; and (5) the laterally extensive nature of individual horizontal reflectors visible in seismic sections at the top of "acoustic basement" (Tamaki, Pisciotto, Allan, et al., 1990). Intrusion likely took place at about 20 Ma for both sites (Kaneoka et al., this volume). Units 1, 2, and 4 from Site 797 were interpreted by Tamaki, Pisciotto, Allan, et al. (1990) to be lava flows, as they lack chilled margins and typically are highly fractured and brecciated.

Units from Sites 794 and 797 have been variably altered, with loss on ignition (LOI) ranging from 1.6% to 8.4% (Tamaki, Pisciotto, Allan, et al., 1990). The interiors of the spinel-bearing lithologic units (lava flows or sills) are moderately to very highly altered ($\approx$30% to 90% replacement minerals), where secondary green- and brown-colored mixed-layer clays, pyrite, and carbonate completely replace olivine and mesostasis and partially replace clinopyroxene and plagioclase. Subophitic, intergranular, coarse interstitial, and coarse microlitic textures were observed in the doleritic to basaltic unit interiors. Some unit interiors are porphyritic; the basalts of Unit 6, Site 794, and Unit 2, Site 797, are sparsely plagioclase-phyric, as is the doleritic interior of Unit 7, Site 797. The interiors of other spinel-bearing units are represented by coarse, aphyric basalts. Clays, zeolites, quartz, pyrite, and carbonate fill vesicles and fractures. The abundance of these secondary minerals increases dramatically from the coarse core to the chilled margin.

Unit margins, very highly to almost totally altered, commonly exhibit a quench mineralogy of euhedral phenocrysts of altered olivine and plagioclase ($\pm$ euhedral Cr-spinel) within formerly glassy, spherulitic, or microlitic groundmasses (Pl. 1). Spinel is abundant in only a few of the units and always represents <<0.1% of the rock volume. Spinel is the only relict magmatic phase, and may occur as either groundmass grains or as inclusions within olivine or plagioclase. The spinel crystals range from several to slightly more than 100 µm in size and range in color from a translucent orange brown to a nearly opaque dark brown. Some spinels from Site 794 show slightly embayed edges on their crystal margins. The sill and flow margins are otherwise composed primarily of green and brown mixed-layer and kaolinitic clays. Clay, carbonate, and adularia commonly replace plagioclase in these unit margins; preliminary electron microprobe analysis suggests that plagioclase in some samples was enriched in Na during alteration. Several units from both sites showed alteration so intense that the spinel was replaced by pyrite and chalcopyrite. Zierenberger et al. (1988) also reported residual Cr-spinel in intensely hydrothermally altered basalts from the Josephine Ophiolite.

Most major elements and all large-ion lithophile elements were mobile during alteration (Allan and Gorton, this volume; Tamaki, Pisciotto, Allan, et al., 1990; see Table 1). MgO and CaO were particularly affected by hydrothermal alteration, exchanging for one another in the development of the mixed-layer clays in accordance with experimental and theoretical studies of mid-ocean ridge basalt (MORB) hydrothermal alteration (Seyfried, 1987; Mottl, 1983; Seyfried and Mottl, 1982; Seyfried and Bischoff, 1979). Unit 5, Site 794 ($\approx$12 m thick), was continuously sampled in the core and thus offers a unique opportunity to see the effects of alteration on rock chemistry. Figure 2 shows the dramatic effect of alteration (as represented schematically by LOI) on bulk-rock MgO content and Mg/(Mg + Fe^{2+}). Conversely, the rock CaO content declined from 9.1% to 2.5% (Tamaki, Pisciotto, Allan, et al., 1990).

Most of the alteration of the Leg 127 units likely occurred during and immediately after intrusion into soft, water-saturated sediments.

Table 1. Whole-rock analyses, Leg 127.

Hole, section, interval (cm) Unit	794C-13R-2, 93–95 6	794D-11R-1, 89–95 6	797C-10R-1, 90–92 2	797C-15R-1, 77–79 5	797C-16R-2, 70–72 5	797C-19R-2, 42–44 7	797C-19R-4, 61–64 13	797C-31R-2, 36–38 1
SiO_2	48.78	48.58	50.16	48.99	48.14	49.14	45.37	50.24
TiO_2	1.21	1.11	1.12	1.22	1.11	0.88	1.06	1.65
Al_2O_3	16.86	16.15	19.08	21.11	19.32	17.97	20.69	14.91
FeO	10.21	10.26	6.75	6.50	6.83	6.47	7.09	9.25
MnO	0.15	0.16	0.41	0.37	0.44	0.28	0.74	0.19
MgO	13.25	12.43	6.21	9.05	8.37	8.12	8.41	6.13
CaO	3.40	7.75	10.85	7.09	10.02	11.57	10.45	10.04
Na_2O	2.65	2.49	3.75	3.67	3.48	3.09	3.55	3.55
K_2O	1.72	0.25	0.11	0.18	0.05	0.07	0.08	0.52
P_2O_5	0.20	0.15	0.14	0.12	0.12	0.08	0.09	0.24
Total	98.43	99.34	98.58	98.3	97.88	97.63	97.53	97.72
LOI	5.56	4.02	2.39	5.02	3.61	2.4	7.86	1.64
Nb	3.2	2	1	ND	1	ND	ND	5.5
Zr	41	41	97	87	8.0	54	62	160
Y	12.2	16	21.2	18.5	18.4	20.5	21.3	33.6
Sr	190	277	302	252	237	179	189	276
Rb	9	0.4	1	2	ND	ND	1	3
Zn	68	47	63	96	7.1	61	65	87
Cu	60	54	89	89	8.5	83	86	59
Ni	132	147	150	140	158	101	106	36
Cr	316	377	272	325	284	317	396	134
V	271	256	214	250	214	200	260	266
Ce	8	18	13	9	13	9	14	40
Ba	89	57	25	25	22	17	12	181
Mg#	0.720	0.680	0.646	0.734	0.708	0.713	0.701	0.568

Note: Chemical analyses from shipboard wavelength-dispersive XRF measurements of whole-rock samples that averaged 20 cm^3 in volume (Don Sims, analyst). Refer to Tamaki, Pisciotto, Allan, et al. (1990) for a discussion of methods and estimated analytical precision. ND = not detected. Mg# = Mg/(Mg + Fe^{2+}), calculated assuming Fe^{3+}/(Fe^{2+} + Fe^{3+}) = 0.1.
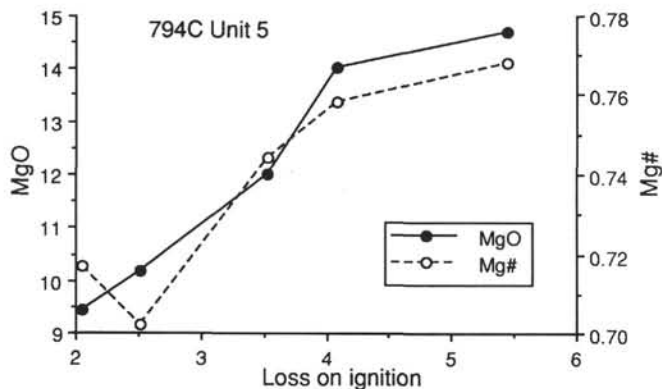

Figure 2. Variation of whole-rock MgO and Mg/(Mg + Fe^{2+}) (Mg#) with loss on ignition for Unit 5, Site 794. Nine meters of continuous core, covering nearly the entire unit thickness, is represented by the data. LOI is used as a proxy for the degree of alteration, with the alteration ranging from 40% to 50% to nearly 100% by volume.

In analogy with similar alteration assemblages present in other hydrothermally altered basalts (Schiffman and Smith, 1988; Franzson et al., 1986), the subgreenschist alteration assemblages indicate temperatures of alteration likely below 230°C. Indeed, Prost et al. (this volume) used oxygen isotope and mineralogical data to determine alteration temperatures of 65° to 180°C for the lowermost units of Site 794. The major element variations are expressed reciprocally in the sediment porewaters above the intrusive units as compared with that exhibited in the intrusive units (i.e., porewater Mg goes down and Ca goes up as sills and flows are approached; Tamaki, Pisciotto, Allan,

et al., 1990). Therefore, these dolerites and basalts serve as both a sink and a source for these elements in the aqueous fluids in the overlying sediments, and at least some of the alteration has taken place during low-temperature (<100°C), ongoing diagenesis.

All spinel-bearing units from both Sites 794 and 797 are interpreted to be tholeiites, based on rock chemistry and quench-margin (near-liquidus) mineralogy. The range in rock chemistry is similar to what has been observed in other backarc basin basalts (e.g., Saunders and Tarney, 1984; Hawkins and Melchior, 1985). At Site 797, two spatially defined geochemical groups were found. The uppermost nine units are incompatible-element-poor tholeiites (Tamaki, Pisciotto, Allan, et al., 1990; Allan and Gorton, this volume). Units 10 through 21 are more enriched in incompatible element content. They range from enriched tholeiites (including the spinel-bearing Unit 13) to mildly alkaline basalts, although alteration makes specific classification difficult (Tamaki, Pisciotto, Allan, et al., 1990). Units from Site 794 are also tholeiitic and differ significantly from MORB only by having moderately to substantially higher Sr (Tamaki, Pisciotto, Allan, et al., 1990; Allan and Gorton, this volume). In particular, the spinel-bearing Unit 6 closely resembles N-type MORB (Pearce et al., 1981).

ANALYTICAL METHODS

Cr-rich spinel was analyzed on a Cameca SX-50 automated electron microprobe, using a finely focused (≈1 μm), nonrastered, spot-fixed electron beam. During analysis, the beam current was 30 nA, and the counting time for all elements was 30 s. Natural mineral standards used included Cr-spinel, ilmenite, and diopside; metal standards were used for analyzing Ni, Zn, and V. Corrections for Ti interference on V were derived by analyzing non-V-containing ilmenite and Ti metal. SiO_2 and CaO were analyzed to determine whether material adjacent to the spinels was inadvertently analyzed.

J. F. ALLAN

Table 2. Representative spinel analyses.

Sample	4-6-2 IC OL	4-6-3 IR OL	4-6-7 IR OL	4-6-8 IC OL	4-6-11 IR OL	4-6-12 IC OL	4-6-13 GC	4-6-15 GR	4-6-16 GC
SiO_2	0.06	0.06	0.06	0.06	0.05	0.05	0.01	0.05	0.04
TiO_2	0.41	0.40	0.49	0.52	0.41	0.47	0.25	0.40	0.30
Al_2O_3	21.13	22.41	28.40	25.25	22.97	22.20	11.96	21.87	19.02
V_2O_3	0.11	0.15	0.18	0.16	0.12	0.08	0.07	0.09	0.10
Cr_2O_3	43.50	41.19	33.56	37.43	41.13	42.61	54.85	40.31	46.25
FeO	20.46	22.45	20.80	20.45	18.74	18.34	20.15	23.69	19.36
MnO	0.13	0.28	0.15	0.16	0.15	0.18	0.16	0.21	0.10
NiO	0.19	0.13	0.10	0.16	0.14	0.17	0.14	0.09	0.19
ZnO	0.02	0.16	0.10	0.04	0.07	0.12	0.06	0.16	0.00
MgO	13.18	12.04	14.18	13.64	14.89	14.72	11.27	11.43	13.34
CaO	0.01	0.02	0.01	0.01	0.01	0.00	0.01	0.02	0.01
Total	99.21	99.27	98.03	97.89	98.68	98.95	98.93	98.32	98.71
$^aFe_2O_3$	5.85	6.13	6.98	6.28	6.72	6.10	4.25	6.80	5.55
^aFeO	15.19	16.93	14.52	14.81	12.69	12.85	16.33	17.58	14.37
Total	99.79	99.88	98.73	98.52	99.35	99.56	99.36	99.00	99.26
Si	0.0019	0.0017	0.0019	0.0019	0.0016	0.0017	0.0002	0.0017	0.0013
Ti	0.0096	0.0094	0.0111	0.0120	0.0094	0.0107	0.0061	0.0094	0.0070
Al	0.7720	0.8200	1.0103	0.9144	0.8273	0.8013	0.4614	0.8115	0.7033
V	0.0028	0.0037	0.0044	0.0039	0.0030	0.0021	0.0019	0.0022	0.0025
Cr	1.0657	1.0107	0.8007	0.9089	0.9930	1.0313	1.4192	1.0030	1.1468
Fe^{3+}	0.1365	0.1433	0.1585	0.1451	0.1545	0.1406	0.1047	0.1610	0.1309
Fe^{2+}	0.3938	0.4396	0.3666	0.3803	0.3242	0.3290	0.4470	0.4627	0.3770
Mn	0.0034	0.0073	0.0039	0.0043	0.0038	0.0046	0.0044	0.0055	0.0026
Ni	0.0048	0.0031	0.0025	0.0039	0.0033	0.0033	0.0037	0.0024	0.0047
Zn	0.0005	0.0037	0.0023	0.0010	0.0015	0.0026	0.0015	0.0038	0.0000
Mg	0.6088	0.5569	0.6376	0.6242	0.6779	0.6717	0.5496	0.5362	0.6236
Ca	0.0003	0.0006	0.0003	0.0003	0.0004	0.0001	0.0003	0.0005	0.0004
Total	3	3	3	3	3	3	3	3	3
$Fe^{3+}/(Cr+Al+Fe^{3+})$	0.069	0.073	0.080	0.074	0.078	0.071	0.053	0.082	0.066
$Cr/(Cr+Al+Fe^{3+})$	0.540	0.512	0.407	0.462	0.503	0.523	0.715	0.508	0.579
$Cr/(Cr+Al)$	0.580	0.552	0.442	0.498	0.546	0.563	0.755	0.553	0.620
$Mg/(Mg+Fe^{2+})$	0.607	0.559	0.635	0.621	0.676	0.671	0.551	0.537	0.623

Note: I = inclusion, C = core, R = rim, OL = in olivine, PL = in plagioclase, G = in groundmass.
^{a} Calculated from the measured FeO (after Carmichael, 1967).

SPINEL CHEMISTRY

The Cr-rich spinels in this study are classified as chromium spinels, magnesiochromites, or chromites using the criteria and terminology of Sigurdsson (1977) and Deer et al. (1962). Their compositions are plotted in Figure 3, and representative analyses are given in Table 2. With the exception of the very Cr-rich core of a single spinel from Unit 6, Site 794, the spinels are similar to other spinels reported from MORBs, MORB-type tholeiites from near-ridge seamounts, and tholeiitic basalts from backarc spreading centers (Dick and Bullen, 1984; Basaltic Volcanism Study Project, 1981; Allan, Sack, and Batiza, 1988; Allan et al., 1987, 1989; Hawkins and Melchior, 1985). Calculated ferric iron contents are low in all of the analyzed spinels (Fe_2O_3 varies from 4.3% to 7.2%, except those of the enriched tholeiite Unit 13, Site 797), similar to other spinels from MORBs (Dick and Bullen, 1984; Basaltic Volcanism Study Project, 1981). TiO_2 is also low in these spinels (below 0.67% in all but the spinels from Unit 13), reflecting the low TiO_2 of the host rock. The higher TiO_2 and $Fe^{3+}/(Cr+Al+Fe^{3+})$ of the Unit 13 spinels is similar to that observed in spinel from enriched MORB (E-MORB; Sun et al., 1979) from the northern Juan de Fuca Ridge area (J. F. Allan et al., unpubl. data) and in spinel from mildly alkaline near-ridge seamount lavas (Batiza and Vanko, 1984). In addition, minor amounts of spinel V_2O_3, MnO, NiO, and ZnO were measured as 0.0% to 0.23%, 0.06% to 0.28%, 0.02% to 0.31%, and 0.0% to 0.33%, respectively.

Spinels from the Site 797 units exhibited only small ranges in composition within individual units (Fig. 3). In addition, analysis by microprobe and backscattered electron imaging show that zoning within individual spinel grains from these units is minor (see core-rim

analysis pairs 7-2-1 and 7-2-2, 7-2-3 and 7-2-4, 7-5-12 and 7-5-13, 7-7-1 and 7-7-2, 7-7-13 and 7-7-14, and 7-13-1 and 7-13-2 in Table 2 and images in Pl. 1).

In contrast, spinel compositions from Unit 6, Site 794, are much more complex. Most of these define a broad band in $Cr/(Cr+Al)$ vs. $Mg/(Mg+Fe^{2+})$ space (Fig. 3), where $Cr/(Cr+Al)$ remains relatively constant while $Mg/(Mg+Fe^{2+})$ changes extensively. Although little zoning is observed in some spinels (e.g., analyses 4-6-11 and 4-6-12, Table 2), others show a significant decrease in $Mg/(Mg+Fe^{2+})$ from core to rim (analyses 4-6-2 and 4-6-3, Table 2), and others show a moderate change in $Cr/(Cr+Al)$ with little change in $Mg/(Mg+Fe^{2+})$ (analyses 4-6-7 and 4-6-8, Table 2). However, one spinel (analyses 4-6-13 and 4-6-15, Table 2, and Pl. 1, Fig. 1) shows sharp zoning in terms of $Cr/(Cr+Al)$. This spinel contains an extremely Cr-rich, Al-poor core that looks slightly rounded in the backscattered electron image. The rim is much more aluminous, similar to other spinels within Unit 6. The core is more Cr-rich and Al-poor than any spinel reported in the literature from a tholeiitic rock.

DISCUSSION

Inference of Magmatic $Mg/(Mg+Fe^{2+})$ From Spinel Composition

Cr-spinel is a complex mineral solution that is best described by reciprocal solution theory (e.g., Wood and Nichols, 1978; Sack, 1982; Sack and Ghiorso, 1991a, 1991b). Accurate description of the solution energetics is requisite if the compositional characteristics of the silicate liquids are to be estimated from the spinel compositions. The crystal chemical model of spinel used here is the ideal reciprocal

Table 2 (continued).

Sample	7-2-1 GC	7-2-2 GR	7-2-3 GC	7-2-4 GR	7-5-1 G	7-5-6 IN PL	7-5-12 GC	7-5-13 GR	7-7-1 GC	7-7-2 GR	7-7-6 GR
SiO_2	0.06	0.10	0.00	0.05	0.23	0.07	0.24	0.09	0.03	0.08	0.05
TiO_2	0.38	0.52	0.41	0.38	0.38	0.40	0.41	0.39	0.64	0.64	0.64
Al_2O_3	40.07	39.34	39.29	38.98	42.83	40.06	39.39	39.11	26.88	28.39	27.37
V_2O_3	0.13	0.00	0.12	0.17	0.05	0.09	0.09	0.11	0.21	0.19	23.0
Cr_2O_3	25.57	24.65	26.28	25.89	22.05	25.80	25.88	25.76	36.76	35.02	36.88
FeO	15.22	17.11	15.65	15.84	14.60	15.64	15.34	15.69	19.08	19.68	19.00
MnO	0.10	0.19	0.07	0.12	0.08	0.08	0.10	0.15	0.13	0.13	0.12
NiO	0.02	0.15	0.18	0.31	0.18	0.14	0.14	0.16	0.09	0.10	0.11
ZnO	0.00	0.00	0.14	0.01	0.33	0.12	0.15	0.11	0.06	0.02	0.02
MgO	17.99	17.05	18.17	18.18	18.58	18.11	18.05	18.07	15.05	15.01	15.27
CaO	0.10	0.16	0.05	0.07	0.04	0.00	0.05	0.06	0.04	0.05	0.03
Total	99.62	99.28	100.34	100.00	99.34	100.52	99.84	99.69	98.97	99.31	99.71
[a]Fe_2O_3	4.68	5.55	5.60	6.04	4.79	5.10	4.88	5.67	6.36	6.48	6.21
[a]FeO	11.01	12.11	10.62	10.40	10.29	11.05	10.94	10.59	13.36	13.85	13.41
Total	100.09	99.83	100.90	100.60	99.82	101.03	100.33	100.26	99.61	99.96	100.33
Si	0.0016	0.0029	0.0000	0.0014	0.0062	0.0019	0.0068	0.0025	0.0010	0.0025	0.0015
Ti	0.0079	0.0109	0.0085	0.0080	0.0078	0.0084	0.0085	0.0082	0.0144	0.0143	0.0144
Al	1.3166	1.3060	1.2864	1.2805	1.3913	1.3069	1.2946	1.2880	0.9499	0.9946	0.9583
V	0.0030	0.0000	0.0027	0.0039	0.0010	0.0020	0.0021	0.0025	0.0051	0.0045	0.0055
Cr	0.5634	0.5487	0.5769	0.5702	0.4803	0.5645	0.5703	0.5688	0.8790	0.8226	0.8658
Fe^{3+}	0.0982	0.1177	0.1170	0.1266	0.0993	0.1062	0.1025	0.1192	0.1434	0.1449	0.1387
Fe^{2+}	0.2566	0.2852	0.2466	0.2424	0.2372	0.2557	0.2552	0.2475	0.3349	0.3442	0.3332
Mn	0.0024	0.0045	0.0016	0.0029	0.0019	0.0019	0.0024	0.0035	0.0033	0.0033	0.0030
Ni	0.0005	0.0035	0.0040	0.0070	0.0039	0.0031	0.0032	0.0035	0.0022	0.0025	0.0027
Zn	0.0000	0.0000	0.0030	0.0002	0.0067	0.0024	0.0031	0.0024	0.0013	0.0005	0.0004
Mg	0.7471	0.7156	0.7520	0.7549	0.7631	0.7470	0.7498	0.7523	0.6723	0.6646	0.6758
Ca	0.0028	0.0049	0.0014	0.0020	0.0012	0.0001	0.0015	0.0016	0.0013	0.0017	0.0008
Total	3	3	3	3	3	3	3	3	3	3	3
$Fe^{3+}/(Cr+Al+Fe^{3+})$	0.050	0.060	0.059	0.064	0.050	0.054	0.052	0.060	0.073	0.074	0.071
$Cr/(Cr+Al+Fe^{3+})$	0.285	0.278	0.291	0.288	0.244	0.285	0.290	0.288	0.443	0.419	0.441
$Cr/(Cr+Al)$	0.300	0.296	0.310	0.308	0.257	0.302	0.306	0.306	0.478	0.453	0.475
$Mg/(Mg+Fe^{2+})$	0.744	0.715	0.753	0.757	0.763	0.745	0.746	0.752	0.667	0.659	0.670

solution model adapted by Allan, Sack, and Batiza (1988) from Sack (1982). This model assumes (1) that there is ideal mixing between Mg and Fe^{2+} in the melt and (2) that the pressure effect on the spinel-liquid equilibrium is negligible over the pressures of interest (<10 kbar), as determined experimentally by Roeder and Reynolds (1991). For these assumptions, a distribution coefficient may be defined for spinel-melt Mg-Fe^{2+} equilibrium:

$$K_D^{Sp-liq} = \left(\frac{X_{Mg^{2+}}^{liquid}}{X_{Fe^{2+}}^{liquid}}\right)\left(\frac{X_{Fe^{2+}}^{spinel}}{X_{Mg^{2+}}^{spinel}}\right). \quad (1)$$

Due to the coupled nature of substitution within spinel, this K_D will change with spinel composition. Following Allan, Sack, and Batiza (1988) and Sack (1982), the Mg-Fe^{2+} exchange between spinel and the silicate liquid may be written:

$$In\ K_D^{SP-LIQ} = -\frac{\Delta \bar{G}_{EX}^{\circ}}{RT} + \frac{\Delta \mu_{23}^{\circ}}{RT}(X_3) + \frac{\Delta \mu_{24}^{\circ}}{RT}(X_4) + \frac{\Delta \mu_{25}^{\circ}}{RT}(X_5) \quad (2)$$

$$\Delta \bar{G}_{EX}^{\circ} = \left(\bar{G}_{MgO}^{\circ\ liq} - \bar{G}_{FeO}^{\circ\ liq}\right) + \left(\bar{G}_{FeAl_2O_4}^{\circ\ Sp} - \bar{G}_{MgAl_2O_4}^{\circ\ Sp}\right),$$

$$\Delta \mu_{23}^{\circ} = \left(\bar{G}_{MgCr_2O_4}^{\circ\ Sp} + \bar{G}_{FeAl_2O_4}^{\circ\ Sp}\right) - \left(\bar{G}_{FeCr_2O_4}^{\circ\ Sp} + \bar{G}_{MgAl_2O_4}^{\circ\ Sp}\right),$$

$$\Delta \mu_{24}^{\circ} = \left(\frac{1}{2}\bar{G}_{Mg_2TiO_4}^{\circ\ Sp} + \bar{G}_{FeAl_2O_4}^{\circ\ Sp}\right) - \left(\frac{1}{2}\bar{G}_{Fe_2TiO_4}^{\circ\ Sp} + \bar{G}_{MgAl_2O_4}^{\circ\ Sp}\right),$$

$$\Delta \mu_{25}^{\circ} = \left(\bar{G}_{MgFe_2O_4}^{\circ\ Sp} + \bar{G}_{FeAl_2O_4}^{\circ\ Sp}\right) - \left(\bar{G}_{Fe_3O_4}^{\circ\ Sp} + \bar{G}_{MgAl_2O_4}^{\circ\ Sp}\right),$$

where

$$X_3 = \frac{1}{2}\eta_{Cr^{3+}}^{Sp}, X_4 = \eta_{n^{4+}}^{Sp}, X_5 = \frac{1}{2}\eta_{Fe^{3+}}^{Sp},$$

and the η_i terms are the number of i cations in a formula unit based on three cations (e.g., Sack, 1982; Hill and Sack, 1987). Given the spinel composition, temperature of crystallization, and the values for ΔG_{EX}°, $\Delta \mu_{23}^{\circ}$, $\Delta \mu_{24}^{\circ}$, and $\Delta \mu_{25}^{\circ}$, the (Mg/Fe^{2+}) ratio of the magma that crystallized the spinels may be explicitly solved for:

$$\left(\frac{Mg^{2+}}{Fe^{2+}}\right)^{liquid} = \left(\frac{Mg^{2+}}{Fe^{2+}}\right)^{spinel} e^{\left((-\Delta \bar{G}_{EX}^{\circ} + \Delta \mu_{23}^{\circ}(X_3) + \Delta \mu_{24}^{\circ}(X_4) + \Delta \mu_{25}^{\circ}(X_5))/RT\right)} \quad (3)$$

Therefore, for the magma,

$$\frac{Mg}{Mg+Fe^{2+}} = 1 - \left(\frac{1}{1+\frac{Mg}{Fe^{2+}}}\right). \quad (4)$$

Values of $\Delta \mu_{23}^{\circ}$, $\Delta \mu_{24}^{\circ}$, and $\Delta \mu_{25}^{\circ}$, determined experimentally by Hill and Sack (1987), are 4.80, 3.5561 + (0.0015698*$T^{\circ}K$), and 6.39 kcal/gfmw, respectively. ΔG_{EX}° may be derived algebraically from the experimentally determined ln K_D for spinel-olivine Mg-Fe^{2+} exchange (e.g., Jamieson and Roeder, 1984; Hill and Sack, 1987) and an assumed K_D olivine-liquid Mg-Fe^{2+} exchange. The commonly accepted value of this K_D for olivine-basaltic liquid exchange is 0.3 (Roeder and Emslie, 1970), whereas most tholeiitic basalts where quench glass has been analyzed yield values that average about 0.27 (Allan et al., 1989; Perfit and Fornari, 1983; Bender et al., 1978). The derived ΔG_{EX}° from these values using the olivine-spinel exchange data of Hill and Sack (1987) is 2.83 and 3.14 kcal/gmfw, respectively, similar to the value of 3.40 ± 0.18 kcal/gmfw determined by Allan,

Table 2 (continued).

Sample	7-7-9 GR	7-7-13 GC	7-7-14 GR	7-13-1 IC OL	7-13-2 IR OL
SiO_2	0.05	0.04	0.04	0.03	0.04
TiO_2	0.51	0.64	0.61	1.81	1.75
Al_2O_3	29.81	28.17	28.42	18.81	18.89
V_2O_3	0.19	0.13	0.16	0.33	0.32
Cr_2O_3	34.14	36.24	35.46	38.33	37.92
FeO	18.95	19.11	19.15	28.66	28.96
MnO	0.17	0.14	0.18	0.20	0.19
NiO	0.12	0.11	0.12	0.04	0.12
ZnO	0.21	0.09	0.10	0.10	0.04
MgO	15.65	15.49	15.20	11.44	11.38
CaO	0.08	0.06	0.20	0.03	0.12
Total	99.88	100.21	99.64	99.76	99.73
[a]Fe_2O_3	6.77	6.52	6.53	10.78	11.19
[a]FeO	12.86	13.24	13.28	18.96	18.89
Total	100.56	100.86	100.29	100.84	100.85
Si	0.0016	0.0013	0.0012	0.0009	0.0013
Ti	0.0112	0.0142	0.0135	0.0427	0.0414
Al	1.0297	0.9778	0.9914	0.6970	0.7001
V	0.0044	0.0030	0.0038	0.0082	0.0080
Cr	0.7910	0.8437	0.8297	0.9526	0.9421
Fe^{3+}	0.1494	0.1445	0.1454	0.2550	0.2646
Fe^{2+}	0.3152	0.3261	0.3286	0.4984	0.4966
Mn	0.0041	0.0034	0.0044	0.0053	0.0052
Ni	0.0029	0.0026	0.0028	0.0009	0.0031
Zn	0.0046	0.0019	0.0023	0.0023	0.0008
Mg	0.6835	0.6797	0.6705	0.5357	0.5329
Ca	0.0025	0.0019	0.0063	0.0010	0.0041
Total	3	3	3	3	3
$Fe^{3+}/(Cr + Al + Fe^{3+})$	0.076	0.074	0.074	0.134	0.139
$Cr/(Cr + Al + Fe^{3+})$	0.401	0.429	0.422	0.500	0.494
$Cr/(Cr + Al)$	0.434	0.463	0.456	0.577	0.574
$Mg/(Mg + Fe^{2+})$	0.684	0.676	0.671	0.518	0.518

Sack, and Batiza (1988) for Cr-spinels in Lamont seamount MORB-type basalt.

Table 3 summarizes the calculated values of rock magmatic $Mg/(Mg + Fe^{2+})$ derived from the Leg 127 spinel compositions using equations (3) and (4) and substituting values for ΔG_{EX}° of 2.83 and 3.14 kcal/gmfw. The crystallization temperature was assumed to be 1200°C (a typical MORB liquidus temperature), except for the more evolved Unit 13, where 1150°C was assumed. Considering the units of Site 797 first, Units 5 and 7 have obviously undergone considerable MgO enrichment during alteration, resulting in an analyzed bulk-rock $Mg/(Mg + Fe^{2+})$ that is substantially higher than could have been in equilibrium with the analyzed spinels. Unit 13 seems to have undergone more modest MgO enrichment during alteration. In contrast, the bulk-rock $Mg/(Mg + Fe^{2+})$ of Unit 2 seems to accurately reflect the original magmatic composition and appears to have been little changed during moderate alteration.

The spinels of Unit 6 at Site 794 reflect a more complex history and exhibit an enormous range of composition. Neglecting the very Cr-rich spinel core (analysis 4-6-16, Table 2 and Fig. 3) discussed earlier, these spinels show broad variation in the divalent cations Mg and Fe^{2+} while showing comparatively little variation in the trivalent cations, when compared with spinels from other natural and experimental basaltic samples (e.g., Allan, Sack, and Batiza, 1988; Allan et al., 1987; Batiza and Vanko, 1984; Hawkins and Melchior, 1985; Sigurdsson and Schilling, 1976; Natland, 1989; Dick and Bryan, 1978; Fisk and Bence, 1980). Predicted values of magmatic $Mg/(Mg + Fe^{2+})$ for this sample range from 0.51 to 0.68, clearly representing either spinel-liquid disequilibrium or else post-crystallization altera-

tion of the spinels themselves. The great variation in the spinel rim compositions indicates that the latter explanation is the most likely. Unlike most other spinels in this study, they exhibit a patchy opaqueness in transmitted light, with what appears to be slight scalloping along some of their sides. The large variation in spinel $Mg/(Mg + Fe^{2+})$ with associated small variation in spinel $Cr/(Cr + Al)$ in the Unit 6 spinels is similar to the reequilibration phenomena of spinel under metamorphic conditions (Roeder et al., 1979; Engi and Evans, 1980; Sack, 1980), where the trivalent cations are less mobile than the divalent cations. In the case of the Site 794 spinels, Mg was preferentially removed from the spinels to the surrounding mixed-layer clays that grew during alteration.

Nevertheless, the spinels exhibiting the highest $Mg/(Mg + Fe^{2+})$ may be used to provide estimates of the maximum allowable magmatic $Mg/(Mg + Fe^{2+})$ of Unit 6. These estimates, given in Table 3, indicate that the analyses of bulk-rock $Mg/(Mg + Fe^{2+})$ reported in Table 1 are substantially higher than the true magmatic composition.

Inference of Magmatic Oxygen Fugacity

Within Cr-rich spinels, Fe^{3+} and Fe^{2+} are found predominantly within octahedral and tetrahedral crystallographic sites, respectively (Sack and Ghiorso, 1991a). The relative composition of these two species in the spinel structure is a complex function of both melt Fe^{3+} and Fe^{2+} and spinel composition, where crystal chemical effects such as those represented in equation (2) must be taken into account. Magma-spinel Fe^{3+}-Fe^{2+} exchange must be modeled in terms of exchanging the components $Fe^{2+} Fe_2^{3+} O^4$ and $FeCr_2O_4$ between spinel and the melt. This approach is
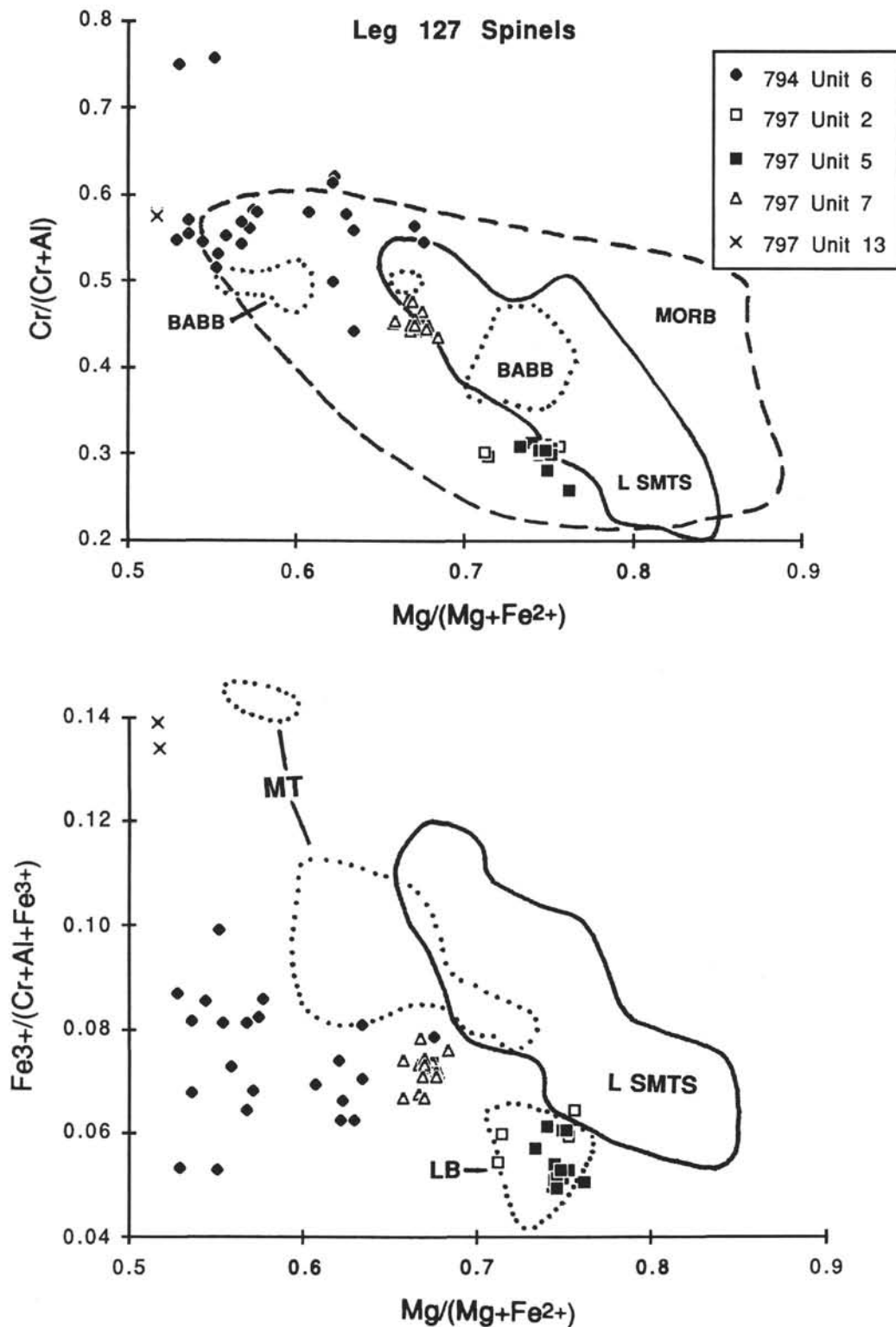
Figure 3. Cr/(Cr + Al) vs. Mg/(Mg + Fe^{2+}) and Fe^{3+}/(Cr + Al + Fe^{3+}) vs. Mg/(Mg + Fe^{2+}) for the Leg 127 Cr-spinels. In the upper graph, the compositional range of MORB Cr-spinel is shown by the dashed line (Dick and Bullen, 1984), compositions of spinel from the Lau Basin and Mariana Trough (Hawkins and Melchior, 1985) backarc basin basalts (BABB) are shown by the dotted lines, and the compositional range of spinels from MORB-type tholeiite erupted from the Lamont seamounts and adjacent East Pacific Rise (Allan, Sack, and Batiza, 1988; Allan et al., 1989) is shown by the solid line (L SMTS). In the lower graph, the BABB field is split into Lau Basin (LB) and Mariana Trough (MT) fields. Most of the Leg 127 Cr-spinels are similar in composition to MORB and BABB spinel; the major exception is the Cr-rich core represented by spinel analysis 4-6-13 in Table 2 and Plate 1, Figure 2. Note the great spread in Mg/(Mg + Fe^{2+}) of the Unit 6, Site 794, spinels, indicating subsolidus Mg-Fe^{2+} exchange with the surrounding rock during hydrothermal and diagenetic alteration.

Table 3. Predicted vs. analyzed Mg/(Mg + Fe²⁺).

Sample	Spinel		Predicted magmatic Mg/(Mg + Fe²⁺)		
	Cr/(Cr + Al)	Mg/(Mg + Fe²⁺)	$\Delta G_{EX}^{\circ} = -2.83$	$\Delta G_{EX}^{\circ} = -3.14$	Analyzed rock Mg/(Mg + Fe²⁺)
Site 794 Unit 6 (23 analyses)	0.44–0.76	0.53–0.68	≈ 0.64–0.68	≈ 0.62–0.66	0.68–0.72
Site 797 Unit 2 (4 analyses)	0.30–0.31	0.71–0.76	0.63–0.69	0.61–0.66	0.65
Site 797 Unit 5 (11 analyses)	0.26–0.32	0.73–0.76	0.65–0.68	0.63–0.66	0.71–0.73
Site 797 Unit 7 (16 analyses)	0.43–0.48	0.66–0.68	0.63–0.66	0.60–0.63	0.70–0.71
Site 797 Unit 13 (2 analyses)	0.57	0.52	0.56	0.53	0.57
56 analyses					

Note: ΔG_{EX}° = −2.83 kcal/gmfw for spinel-liquid Mg-Fe²⁺ exchange calculated assuming K_D = 0.3 for Mg-Fe²⁺ exchange between olivine and silicate liquid (Roeder and Emslie, 1970). ΔG_{EX}° = −3.14 kcal/gmfw for spinel-silicate liquid Mg-Fe²⁺ exchange calculated assuming K_D = 0.27 for Mg-Fe²⁺ exchange between olivine and silicate liquid (Allan et al., 1989). Analyzed rock Mg/(Mg + Fe²⁺) calculated assuming Fe³⁺/(Fe³⁺ + Fe²⁺) = 0.1.

problematical, as fO₂ directly affects not only magmatic Fe³⁺/Fe²⁺ but also magmatic Cr³⁺/Cr²⁺ (Roeder and Reynolds, 1991; Schreiber, 1977, 1987; Schreiber and Haskin, 1976). Magmatic fO₂ is itself a function of both magma Fe³⁺/Fe²⁺ and chemical composition (Sack et al., 1980; Kilinc et al., 1983; Schreiber, 1987; Thornber et al., 1980; Fudali, 1965). Roeder and Reynolds (1991) assumed constant melt-spinel Cr³⁺/Cr²⁺ and showed that linear regression of their experimental results on melt-spinel equilibria could produce estimates of magmatic fO₂ when the composition of both spinel and the melt were known. Other methods of inferring magmatic fO₂ have utilized coexisting oxides (e.g., Buddington and Lindsley, 1964) or coexisting oxides and silicate phases (Mattioli and Wood, 1988). However, when the composition of the liquid is unknown, spinel is the only magmatic phase present containing Fe³⁺, and the composition of all other phases is unknown, direct inference of magmatic fO₂ from spinel ferric-ferrous compositions is impossible.

Nevertheless, experimental studies indicate broad relationships between magmatic fO₂ and spinel Fe³⁺, Fe²⁺, and spinel Fe³⁺/(Fe³⁺ + Fe²⁺). Roeder and Reynolds (1991) and Fisk and Bence (1980) found that spinel Fe³⁺/(Al + Cr + Fe³⁺) is positively correlated with melt fO₂ for a given melt composition, with the increase in spinel Fe³⁺ reflecting a decrease in spinel Cr but only a slight decrease in Al (Roeder and Reynolds, 1991). This relationship reflects the reciprocal nature of the spinel crystal chemistry, where Fe²⁺ is more strongly coupled to Cr and Fe³⁺ than it is to Al (Sack, 1982). In addition, spinel Fe³⁺ and Fe³⁺/Fe²⁺ were found to increase with decreasing temperature. Figures 3 and 4 compare Leg 127 spinel Fe³⁺/(Fe³⁺ + Fe²⁺) and Fe³⁺/(Fe³⁺ + Fe²⁺) with that of spinels from other oceanic basalts. For two of these suites (N-type MORBs from the Lamont seamounts and hawaiites from the Tuzo Wilson seamounts), FeO contents have been directly determined on glass coexisting with spinel (Allan, Sack, and Batiza, 1988; Allan et al., 1989; Allan, Cousens, et al., 1988; J. F. Allan et al., unpubl. data), allowing a calculation of glass Fe³⁺/Fe²⁺ and an estimation of magmatic fO₂ (Sack et al., 1980; Kilinc et al., 1983). These two suites were calculated to have had magmatic oxygen fugacities of 1.0–1.8 and 0–1.0 log units below the nickel–nickel oxide (NNO) buffer (Huebner and Sato, 1970), respectively, with the Lamont suite similar in fO₂ to other MORB tholeiites (Christie et al., 1986). The low Fe³⁺/(Cr + Al + Fe³⁺) and Fe³⁺/(Fe³⁺ + Fe²⁺) of the Leg 127 spinels (Figs. 3 and 4) imply that the Leg 127 spinels crystallized at reduced conditions similar to MORBs, with the more reduced upper suite from Site 797 (Units 2, 5, and 7) likely several log units below the NNO buffer.

Implications of the Zoned Unit 6 Spinel

One large spinel found in Unit 6, Site 794, exhibited sharp compositional zoning in Cr/(Cr + Al) (analyses 4-6-13 and 4-6-15, Table 2) easily visible in backscattered electron imagery (Pl. 1). This sharp zoning is strong evidence for marked disequilibrium between the spinel core and the host silicate liquid during eruption (Allan, Sack, and Batiza, 1988), as the rim of the spinel is similar in Cr/(Cr + Al) composition to the other analyzed spinels in the unit. In contrast, the spinel core composition plots well outside of published MORB and backarc basin basalt (BABB) fields (Fig. 3). Several studies (Allan, Sack, Batiza, 1988; Fisk and Bence, 1980; Sigurdsson and Schilling, 1976) have shown that the Al₂O₃ of Ti-poor Cr-spinel is directly related to the Al₂O₃ of the host silicate liquid (as represented by glass). If this spinel crystallized from a melt, then the parental magma must have had substantially lower Al₂O₃ than MORBs, as well as had a very low TiO₂ content. Similar spinel compositions have been reported from low-Al₂O₃, high-MgO arc-related andesites and boninites (Dick and Bullen, 1984), including a magnesian andesite from southwest Japan (Tatsumi and Ishizaka, 1981). Alternatively, the low-Al core might represent a xenocryst derived from dunite depleted by melt extraction (T. Fujii, pers. comm., 1990), with the spinel Mg/(Mg + Fe²⁺) reduced during alteration. This zoned spinel provides direct evidence for the presence of other unsampled rock types in the Yamato Basin and could reflect magma mixing of a boninitic or low-Al₂O₃ andesitic magma with a tholeiitic magma prior to eruption, or wall-rock assimilation of previously erupted material. The lack of other xenoliths indicates that magma mixing is the more feasible explanation.

CONCLUSIONS

1. Cr-spinels preserved in highly altered basaltic sills and flows contain valuable evidence that uniquely allow for the determination of critical magmatic compositional characteristics, Mg/(Mg + Fe²⁺) in particular.

2. Leg 127 spinel compositions were used with thermodynamic equations assuming spinel reciprocal solution behavior and ideal mixing to determine host magmatic Mg/(Mg + Fe²⁺) directly. These calculations show that some of the Leg 127 igneous units underwent substantial enrichment in MgO during hydrothermal and diagenetic alteration, resulting in bulk-rock Mg/(Mg + Fe²⁺) values higher than were present in the original magma.

3. Comparison of the spinel compositions with others from fresh basalts confirmed the impression, based upon whole-rock analyses, that
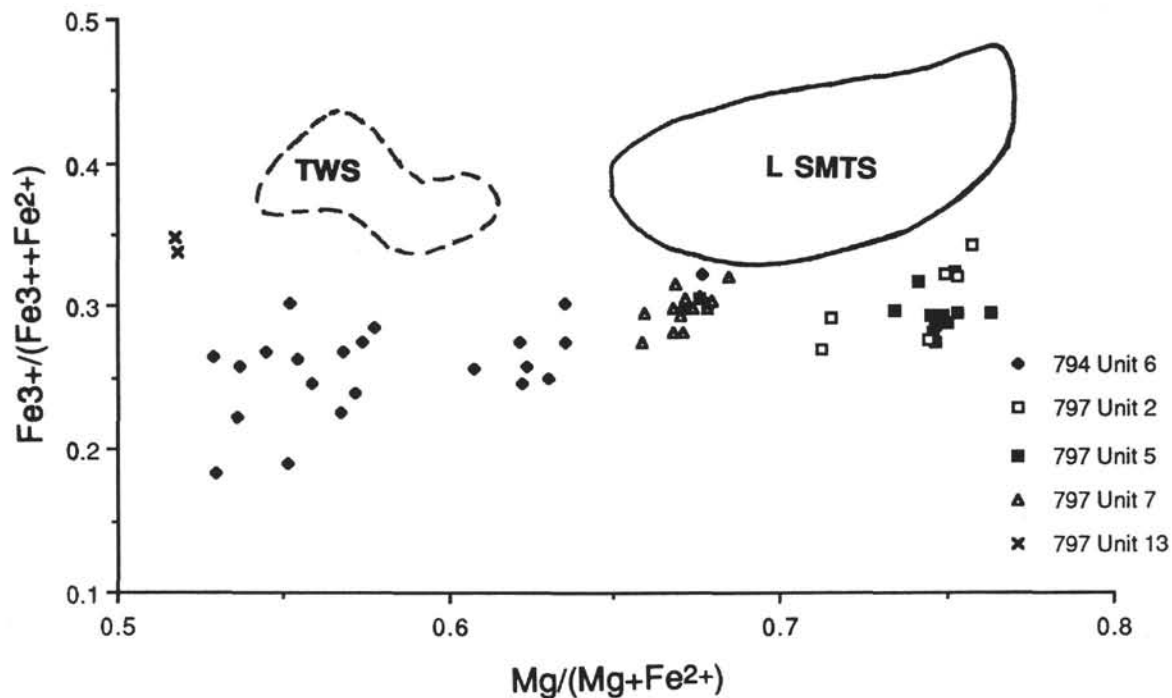
Figure 4. Spinel $Fe^{3+}/(Fe^{3+} + Fe^{2+})$ vs. $Mg/(Mg + Fe^{2+})$ in the Leg 127 units. Also shown are ranges in spinel compositional values from the Lamont seamounts (L SMTS = solid line; Allan, Sack, and Batiza, 1988; Allan et al., 1989) and the Tuzo Wilson seamounts, west of British Columbia (TWS = dashed line; Allan, Cousens, et al., 1988; J. F. Allan and R. Chase, unpubl. data). Analyzed spinels from the Lamont and Tuzo Wilson seamounts occur in quench glass analyzed for FeO by wet chemical means (I.S.E. Carmichael, analyst), which allow for a precise determination of magmatic fO_2. With the exception of spinels from Unit 13, Site 797, the Leg 127 spinels fall well below these two suites in $Fe^{3+}/(Fe^{3+} + Fe^{2+})$, indicating that they crystallized at magmatic fO_2 of 2 or more log units below the nickel–nickel oxide buffer.

the host magmas were tholeiitic and similar to MORBs or BABBs, with most crystallizing under conditions of low fO_2 (2 log units or more below the NNO buffer). However, a strongly zoned spinel with a Cr-rich, Al-poor core provides direct evidence for the presence of unsampled, low-Al igneous rocks in the crust of the Yamato Basin, with possible rock types including boninite and high-Mg andesite.

ACKNOWLEDGMENTS

REFERENCES

Allan, J. F., Batiza, R., and Lonsdale, P., 1987. Petrology of lavas from seamounts flanking the East Pacific Rise axis, 21°N: implications concerning the mantle source composition for both seamount and adjacent EPR lavas. *In* Keating, B., Fryer, I., Batiza, R., and Boehlert, G. W. (Eds.), *Seamounts, Islands, and Atolls*. Am. Geophys. Union, Geophys. Monogr., 43:255–282.

Allan, J. F., Batiza, R., Perfit, M. R., Fornari, D. J., and Sack, R. O., 1989. Petrology of lavas from the Lamont seamount chain and adjacent East Pacific Rise, 10°N. *J. Petrol.*, 30:1245–1298.

Allan, J. F., Cousens, B., Chase, R., and Gorton, M., 1988. Alkaline lavas from the Tuzo Wilson seamounts, NE Pacific: volcanism at a complex oceanic ridge-transform fault intersection. *Eos*, 69:1503.

Allan, J. F., Sack, R. O., and Batiza, R., 1988. Cr-rich spinels as petrogenetic indicators: MORB-type lavas from the Lamont seamount chain, eastern Pacific. *Am. Mineral.*, 73:741–753.

Basaltic Volcanism Study Project, 1981. *Basaltic Volcanism on the Terrestrial Planets*: New York (Pergamon).

Batiza, R., and Vanko, D., 1984. Petrology of young Pacific seamounts. *J. Geophys. Res.*, 89:11235–11260.

Bender, J. F., Hodges, F. N., and Bence, A. E., 1978. Petrogenesis of basalts from the project FAMOUS area: an experimental study from 0 to 15 kbars. *Earth Planet. Sci. Lett.*, 41:277–302.

Buddington, A. F., and Lindsley, D. H., 1964. Iron-titanium oxide minerals and synthetic equivalents. *J. Petrol.*, 5:310–357.

Carmichael, I.S.E., 1967. The iron-titanium oxides of salic volcanic rocks and their associated ferromagnesian silicates. *Contrib. Mineral. Petrol.*, 14:36–64.

Celaya, M., and McCabe, R., 1987. Kinematic opening of the Sea of Japan and the bending of the Japanese Islands. *Geology*, 15:53–57.

Christie, D. M., Carmichael, I.S.E., and Langmuir, C. H., 1986. Oxidation states of mid-ocean ridge basalt glasses. *Earth Planet. Sci. Lett.*, 79:397–411.

Deer, W. A., Howie, R. A., and Zussman, J., 1962. *Rock Forming Minerals* (Vol. 5): *Non-Silicates*: London (Longman).

Dick, H.J.B., and Bryan, W. B., 1978. Variation of basalt phenocryst mineralogy and rock compositions in DSDP Hole 396B. *In* Dmitriev, L., Heirtzler, J., et al., *Init. Repts. DSDP*, 46: Washington (U.S. Govt. Printing Office), 215–225.

Dick, H.J.B., and Bullen, T., 1984. Chromium spinel as a petrogenetic indicator in abyssal and alpine-type peridotites and spatially associated lavas. *Contrib. Mineral. Petrol.*, 86:54–76.

Engi, M., and Evans, B. W., 1980. A re-evaluation of the olivine-spinel geothermometer: discussion. *Contrib. Mineral. Petrol.*, 73:201–203.

Fisk, M. R., and Bence, A. E., 1980. Experimental crystallization of chrome spinel in FAMOUS basalt 527-1-1. *Earth Planet. Sci. Lett.*, 48:111–123.

Foruta, T., and Tokuyama, H., 1983. Chromium spinels in Costa Rica basalts, Deep Sea Drilling Project Site 505—a preliminary interpretation of electron microprobe analyses. *In* Cann, J. R., Langseth, M. G., Honnorez, J., Von Herzen, R. P., White, S. M., et al., *Init. Repts., DSDP,* 69: Washington (U.S. Govt. Printing Office), 805–810.

Franzson, H., Gudmundsson, A., Fridleifsson, G. O., and Tomasson, J., 1986. Nesjavellir high-T field, SW-Iceland: reservoir geology. *Proc. 5th International Symp. Water-Rock Interaction.* Int. Assoc. Geochem. Cosmochem., 210–213.

Fudali, R. F., 1965. Oxygen fugacities of basaltic and andesitic magmas. *Geochim. Cosmochim. Acta,* 29:1063–1075.

Hawkins, J. W., and Melchior, J. T., 1985. Petrology of Mariana Trough and Lau Basin basalts. *J. Geophys. Res.,* 90:11431–11468.

Hilde, T. W., and Wageman, J. M., 1973. Structure and origin of the Japan Sea. *In* Coleman, P. J. (Ed.), *The Western Pacific: Island Arcs, Marginal Seas, Geochemistry:* Perth (Univ. of Western Australia Press), 415–434.

Hill, R. L., and Sack, R. O., 1987. Thermodynamic properties of Fe-Mg titanomagnetite spinels. *Can. Mineral.,* 25:443–464.

Huebner, J. S., and Sato, M., 1970. The oxygen-temperature relationships of manganese oxide and nickel oxide buffers. *Am. Mineral.,* 55:934–952.

Ingle, J. C., Jr., Suyehiro, K., von Breymann, M. T., et al., 1990. *Proc. ODP, Init. Repts.,* 128: College Station, TX (Ocean Drilling Program).

Irvine, T. N., 1965. Chrome spinel as a petrogenetic indicator. Part 1: theory. *Can. J. Earth Sci.,* 2:648–672.

————, 1967. Chromium spinel as a petrogenetic indicator. Part 2: petrological applications. *Can. J. Earth Sci.,* 4:71–103.

————, 1976. Chromite crystallization in the join Mg_2SiO_4-$CaMgSi_2O_6$-$CaAl_2Si_2O_8$-$MgCr_2O_4$-SiO_2. *Year Book—Carnegie Inst. Washington,* 76:465–472.

Jamieson, H. E., and Roeder, P. L., 1984. The distribution of Mg and Fe^{2+} between olivine and spinel at 1300°C. *Am. Mineral.,* 69:283–291.

Karig, D. E., 1971. Origin and development of marginal basins in the western Pacific. *J. Geophys. Res.,* 76:2542–2561.

————, 1974. Evolution of arc systems in the western Pacific. *Annu. Rev. Earth Planet. Sci.,* 2:51–75.

Kilinc, A., Carmichael, I.S.E., Rivers, M. L., and Sack, R. O., 1983. The ferric-ferrous ratio of natural silicate liquids equilibrated in air. *Contrib. Mineral. Petrol.,* 83:136–140.

Lallemand, S., and Jolivet, L., 1986. Japan Sea: a pull-apart basin? *Earth Planet. Sci. Lett.,* 76:375–389.

Mattioli, G. S., and Wood, B. J., 1988. Magnetite activities across the $MgAl_2O_4$-Fe_3O_4 spinel join, with application to thermobarometric estimates of upper mantle oxygen fugacity. *Contrib. Mineral. Petrol.,* 98:148–162.

Mottl, M. J., 1983. Metabasalts, axial hot springs, and the structure of hydrothermal systems at mid-ocean ridges. *Geol. Soc. Am. Bull.,* 94:161–180.

Natland, J. H., 1989. Partial melting of a lithologically heterogeneous mantle: inferences from crystallization histories of magnesian abyssal tholeiites from the Siqueiros Fracture Zone. *In* Saunders, A. D., and Norry, M. J. (Eds.), *Magmatism in the Ocean Basins.* Geol. Soc. Spec. Publ. London, 42:41–70.

Natland, J. H., Adamson, A. C., Laverne, C., Melson, W. G., and O'Hearn, T., 1983. A compositionally nearly steady-state magma chamber at the Costa Rica Rift: evidence from basalt glass and mineral data. Deep Sea Drilling Project Sites 501, 504, and 505. *In* Cann, J. R., Langseth, M. G., Honnorez, J., Von Herzen, R. P., White, S. M., et al., *Init. Repts. DSDP,* 69: Washington (U.S. Govt. Printing Office), 811–858.

Pearce, J. A., Alabaster, T., Shelton, A. W., and Searle, M. P., 1981. The Oman Ophiolite as a Cretaceous arc-basin complex: evidence and implications. *Philos. Trans. R. Soc. London A,* 300:299–317.

Perfit, M. R., and Fornari, D. J., 1983. Geochemical studies of abyssal lavas recovered by DSRV *ALVIN* from Eastern Galapagos Rift, Inca Transform, and Ecuador Rift 2. Phase chemistry and crystallization history. *J. Geophys. Res.,* 88:10530–10550.

Roeder, P. L., Campbell, I. H., and Jamieson, H. E., 1979. A re-evaluation of the olivine-spinel geothermometer. *Contrib. Mineral. Petrol.,* 68:325–334.

Roeder, P. L., and Emslie, R. F., 1970. Olivine-liquid equilibrium. *Contrib. Mineral. Petrol.,* 29:275–289.

Roeder, P. L., and Reynolds, I., 1991. Crystallization of chromite and chromium solubility in basaltic liquid. *J. Petrol.,* 32:909–934.

Sack, R. O., 1980. Adirondack mafic granulites and a model lower crust: summary. *Geol. Soc. Am. Bull.,* 91 (Pt. 1):89–93.

————, 1982. Spinels as petrogenetic indicators: activity-composition relations at low pressures. *Contrib. Mineral. Petrol.,* 79:169–186.

Sack, R. O., Carmichael, I.S.E., Rivers, M. L., and Ghiorso, M. S., 1980. Ferric-ferrous equilibria in natural silicate liquids at 1 bar. *Contrib. Mineral. Petrol.,* 75:369–376.

Sack, R. O., and Ghiorso, M. S., 1991a. Chromian spinels as petrogenetic indicators: thermodynamics and petrological applications. *Am. Mineral.,* 76:827–847.

————, 1991b. An internally consistent model for the thermodynamic properties of Fe-Mg-titanomagnetite-aluminate spinels. *Contrib. Mineral. Petrol.,* 106:474–505.

Saunders, A. D., and Tarney, J., 1984. Geochemical characteristics of basaltic volcanism within back-arc basins. *In* Kokelaar, B. P., and Howells, M. F., (Eds.), *Marginal Basin Geology:* London (Blackwell Sci.), 59–76.

Schiffman, P., and Smith, B. M., 1988. Petrology and oxygen isotope geochemistry of a fossil seawater hydrothermal system within the Solea Graben, Northern Troodos Ophiolite, Cyprus. *J. Geophys. Res.,* 93:4612–4624.

Schreiber, H. D., 1977. Redox states of Ti, Zr, Hf, Cr, and Eu in basaltic magmas: an experimental study. *Proc. Lunar Sci. Conf.,* 8:1785–1807.

————, 1987. An electrochemical series of redox couples in silicate melts: a review and applications to geochemistry. *J. Geophys. Res.,* 92:9225–1295.

Schreiber, H. D., and Haskin, L. A., 1976. Chromium in basalts: experimental determination of redox states and partitioning among synthetic silicate phases. *Proc. Lunar Sci. Conf.,* 7:1221–1259.

Scowen, P. A., Roeder, P. L., and Helz, R. T., 1991. Reequilibration of chromite within Kilauea Iki lava lake, Hawaii. *Contrib. Mineral. Petrol.,,* 107:8–20.

Seyfried, W. E., Jr., 1987. Experimental and theoretical constraints on hydrothermal alteration processes at mid-ocean ridges. *Annu. Rev. Earth Planet. Sci.,* 15:317–335.

Seyfried, W. E., Jr., and Bischoff, J. L., 1979. Low temperature basalt alteration by seawater: an experimental study at 70°C and 150°C. *Geochim. Cosmochim. Acta,* 43:1937–1947.

Seyfried, W. E., Jr., and Mottl, M. J., 1982. Hydrothermal alteration of basalt by seawater under seawater-dominated conditions. *Geochim. Cosmochim. Acta,* 46:985–1002.

Sigurdsson, H., 1977. Spinels in Leg 37 basalts and peridotites: phase chemistry and zoning. *In* Aumento, F., Melson, W. G., et al., *Init. Repts. DSDP,* 37: Washington (U.S. Govt. Printing Office), 883–891.

Sigurdsson, H., and Schilling, J.-G., 1976. Spinels in Mid-Atlantic Ridge basalts: chemistry and occurrence. *Earth Planet. Sci. Lett.,* 29:7–20.

Sun, S. S., Nesbitt, R. W., and Sharaskin, A. Y., 1979. Geochemical characteristics of mid-ocean ridge basalts. *Earth Planet. Sci. Lett.,* 44:119–138.

Tamaki, K., 1985. Two modes of back-arc spreading. *Geology,* 13:475–478.

Tamaki, K., Pisciotto, K., Allan, J., et al., 1990. *Proc. ODP, Init. Repts.,* 127: College Station, TX (Ocean Drilling Program).

Tatsumi, I., and Ishizaka, K., 1981. Existence of andesitic primary magma: an example from S.W. Japan. *Earth Planet. Sci. Lett.,* 53:124–130.

Thornber, C. R., Roeder, P. L., and Foster, J. R., 1980. The effect of composition on the ferric-ferrous ratio in basaltic liquids at atmospheric pressure. *Geochim. Cosmochim. Acta,* 44:525–532.

Wood, B. J., and Nicholls, J., 1978. The thermodynamic properties of reciprocal solid solutions. *Contrib. Mineral. Petrol.,* 66:389–400.

Zierenberg, R. A., Shanks, W. C., III, Seyfried, W. E., Jr., Koski, R. A., and Strickler, M. D., 1988. Mineralization, alteration, and hydrothermal metamorphism of the ophiolite-hosted Turner-Albright sulfide deposit, southwestern Oregon. *J. Geophys. Res.,* 93:4657–4674.
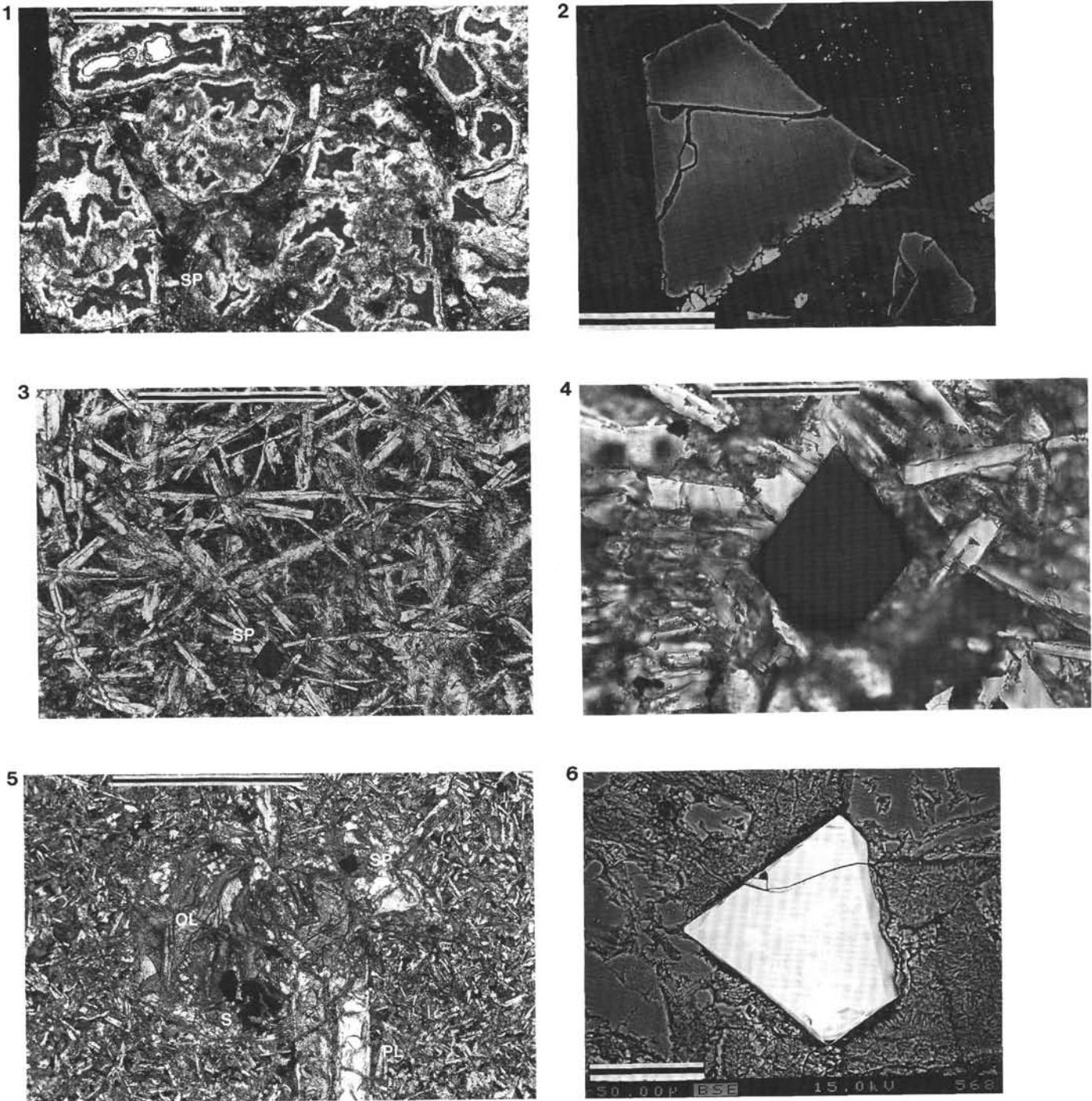
Plate 1. Photomicrographs of Leg 127 spinels showing their euhedral shape and the textural relationships in which they are found. **1.** Unit 6, Site 794, spinels occurring either as inclusions within olivine (OL) altered to greenish brown and brown (inner, dark rings) mixed-layer clays or within a formerly spherulitic to microlitic groundmass replaced by mixed-layer clays and kaolinite. SP lies next to the strongly zoned spinel represented by analyses 4-6-13 and 4-6-15 in Table 2. The plagioclase laths have been replaced by K-feldspar adularia. Scale bar = 1 mm. Photograph taken in nonpolarized transmitted light; note the opaque nature of the spinels. **2.** Backscattered electron image of the strongly zoned spinel denoted by SP in Figure 1. The lighter, Cr-rich core is sharply zoned to a darker, more Al-rich rim. Scale bar = 50 μm. **3.** Unit 2, Site 797, spinel (SP) in microlitic groundmass. The spinel represents analyses 7-2-3 and 7-2-4 in Table 2. Scale bar = 0.5 mm. Photograph taken in nonpolarized transmitted light; note the translucent nature of the spinel. **4.** Close-up of the spinel in Figure 3. Scale bar = 0.1 mm. Photograph taken in nonpolarized transmitted and reflected light; note the sharply euhedral nature of the spinel. **5.** Unit 13, Site 797, spinel (SP) representing analyses 7-13-1 and 7-13-2 in Table 2. Spinel occurs with olivine (OL) replaced by green-brown mixed-layer clays, carbonate, and sulfide (S: pyrite or marcasite). Associated with the olivine is a plagioclase phenocryst (PL) that has a core replaced by carbonate, with an An_{32-44} rim composition that may have been affected by Na loss. Scale bar = 1 mm. **6.** Backscattered electron image of spinel in Figure 5. Scale bar = 50 μm. Note the unzoned nature of the spinel and its sharp, euhedral outline.